Doping-dependence of nodal quasiparticle properties in high-T_c cuprates studied by laser-excited angle-resolved photoemission spectroscopy

K. Ishizaka,[1] T. Kiss,[1] S. Izumi,[1] M. Okawa,[1] T. Shimojima,[1] A. Chainani,[2] T. Togashi,[2] S. Watanabe,[1] C.-T. Chen,[3] X. Y. Wang,[3] T. Mochiku,[4] T. Nakane,[4] K. Hirata,[4] and S. Shin[1,2]

[1]*Institute for Solid State Physics, University of Tokyo, Kashiwa, Chiba 277-8581, Japan*
[2]*The Institute of Physical and Chemical Research (RIKEN), Sayo-gun, Hyogo 679-5143, Japan*
[3]*Beijing Center for Crystal R&D, Chinese Academy of Sciences, Zhongguancun, Beijing 100080, People's Republic of China*
[4]*National Institute for Materials Science, Tsukuba, Ibaraki 305-0047, Japan*

We investigate the doping dependent low-energy, low temperature ($T=5$ K) properties of nodal quasiparticles in the d-wave superconductor $Bi_{2.1}Sr_{1.9}CaCu_2O_{8+\delta}$ (Bi2212). By utilizing ultrahigh resolution laser-excited angle-resolved photoemission spectroscopy, we obtain precise band dispersions near E_F, mean free paths, and scattering rates (Γ) of quasiparticles. For optimally and overdoped samples, we obtain very sharp quasiparticle peaks of 8 and 6 meV full width at half maximum, respectively. The value of Γ for optimally doped sample is in good accordance with terahertz conductivity. For all doping levels, we find the energy dependence of $\Gamma \sim |\omega|$, while $\Gamma(\omega=0)$ shows a monotonic increase from overdoping to underdoping. The doping-dependence suggests the role of electronic inhomogeneity on the nodal quasiparticle scattering at low temperature (5 K $\lesssim 0.07 T_c$) pronounced in the underdoped region. The quasiparticle peak spectra match well with a single Lorentzian function, thus indicating that the nodal carriers can be described as well-defined quasiparticles, even in the underdoped region.

PACS number(s): 74.72.Hs, 74.25.Jb, 79.60.−i

Extensive studies over the past two decades have indicated a $d_{x^2-y^2}$ symmetry of the superconducting gap in the Bi-based high-T_c cuprates.[1,2] The $d_{x^2-y^2}$-wave superconducting state is characterized by line nodes along the $(\pm \pi/2, \pm \pi/2)$ direction and allows the existence of quasiparticles crossing the Fermi level even in the gapped superconducting ground state. Early in the literature, theoretical studies have discussed the behavior of nodal quasiparticles in terms of massless fermions with a Dirac-cone dispersion.[3] By investigating such nodal quasiparticles which are responsible for the low-energy excitations, one can acquire insight into the characteristic features of the scattering and interaction mechanisms remaining in the superconducting state. Experimentally, the properties of nodal quasiparticles in the superconducting state can be obtained from transport measurements, such as thermal Hall conductivity,[4] microwave, and terahertz conductivity.[5,6] These studies in $YBa_2Cu_3O_7$ (Y123) had revealed a rapid increase of the quasiparticle lifetime on cooling across the superconducting transition,[4,5] and the mean free path obtained by the thermal Hall conductivity at the lowest temperature attains a value of ~ 1 μm.[4] On the other hand, terahertz conductivity in Bi2212 shows a scattering rate with rather high values and a slower T-linear dependence below T_c compared to Y123.[6] Such differences have been discussed in terms of possible impurity effects, which may accompany phase fluctuations, charge and superfluid density inhomogeneity, etc.

Angle-resolved photoemission spectroscopy (ARPES) is a powerful method to investigate the momentum-resolved nodal quasiparticle properties, both as a function of temperature and energy (ω). The energy position of the quasiparticle peak in ARPES represents the band dispersion, whereas the width indicates the scattering rate Γ. Recent studies have carefully probed the "kink" structure at around 60 meV in the quasiparticle dispersion, now commonly observed in hole-doped cuprates.[2,7] The kink accompanies a rapid decrease of the scattering rate and is discussed as the renormalization of a bosonic mode derived from phonons or magnons.[8–10] There are important studies[2,12,13] that discuss the nature of the scattering mechanism of the electrons from the ω dependence of the scattering rate, e.g, is it a Fermi liquid (with $\Gamma \propto \omega^2$) or a marginal Fermi liquid? (with $\Gamma \propto |\omega|$).[11] Due to limitations of momentum and energy resolutions, however, the low temperature Γ at $\omega=0$ (i.e., the Fermi level) has not been obtained accurately enough to discuss the nodal quasiparticle properties in terms of unique elementary excitations in the d-wave superconducting state. In particular, to date, the discrepancies obtained in its values by transport measurements and ARPES remain to be conclusively clarified. Accordingly, its doping-dependence at low energy and low temperature is also not yet clarified and remains an open question. In this study, we investigate the character of nodal quasiparticles of Bi2212 as a function of doping by vuv laser-excited ARPES measurements. By using a low-energy ($h\nu=6.994$ eV) and coherent light source, we can achieve high energy and momentum resolutions ($\lesssim 1$ meV and 0.0016 Å), as well as bulk sensitivity (~ 100 Å). From our measurements, we obtained a very sharp quasiparticle peak of 6 meV and 0.0039 Å^{-1} full width at half maximum for an overdoped sample. The scattering rate obtained from the quasiparticle peak width shows a clear doping-dependence, increasing monotonically from the overdoped to the underdoped region, reminiscent of the pseudogap phenomenon. The quasiparticle peak spectra match single Lorentzian function curves nicely, thus indicating that the nodal carriers behave as very well-defined quasiparticles, even in the highly correlated underdoped region.

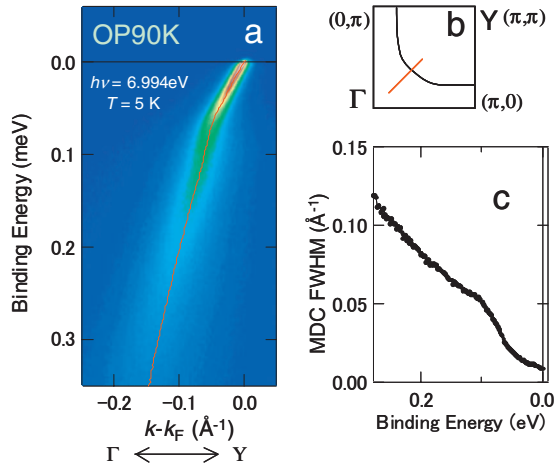ARPES measurements were performed using a system

FIG. 1. (Color) (a) ARPES intensity image plot from Bi2212 OP90K. The red curve shows the band dispersion as obtained from the MDC peak positions. (b) A schematic of the Brillouin zone of Bi2212. The red line shows the momentum region of the measurement [along $(0,0)$-(π,π)]. (c) E_B dependence of the MDC FWHM obtained from OP90K.

constructed with a VG-Scienta R4000 electron analyzer and an ultraviolet ($h\nu$=6.994 eV) laser for the incident light.[14] The temperature was precisely controlled down to 5 K using a flow-type He liquid refrigerator. The pressure of the chamber was below $\sim 5\times10^{-11}$ Torr throughout all the measurements. The energy and angular resolutions were E_{res} =1.0 meV and θ_{res}=0.1°. The Fermi level (E_F) of the sample was referred to that of a Au film evaporated on the sample substrate, with an accuracy of ±0.1 meV. High quality single crystals of Bi2212 were grown by the traveling-solvent floating-zone method.[15] T_c of the samples from underdoped to overdoped region were 72 K (UN72K), 80 K (UN80K), 90 K (OP90K), 85 K (OV85K), and 73 K (OV73K). The samples were cleaved *in situ* to obtain clean surfaces. All the data presented in this work were obtained at 5 K.

Figure 1(a) shows the ARPES intensity image along the nodal direction [Γ-Y, see Fig. 1(b) for a schematic Brillouin

zone] from OP90K. As is well known,[2] the kink structure reflecting the band renormalization at ~60 meV is clearly observed in the raw data. To discuss the detailed features appearing in the band dispersion, we performed a fitting analysis of momentum distribution curves (MDCs) (momentum profile of the ARPES intensity at a fixed binding energy) using the sum of a Lorentzian peak and a constant background. The obtained peak positions are overlaid as a red curve in Fig. 1(a) and the full width half maximum (FWHM) Δk is plotted as a function of binding energy (E_B) in Fig. 1(c). Δk thus obtained can be approximately described by $\Delta k\approx 2\,\mathrm{Im}\,\Sigma/v_0$, where v_0 and Σ correspond to the bare Fermi velocity and the self-energy of electrons.[2] Here, Im Σ is related to the scattering rate or inverse of the lifetime of the electrons. The 60 meV kink is easily identified as the knee in the band dispersion, which has been extensively discussed as a renormalization effect due to a bosonic mode. In addition, a rapid decrease of Δk at lower binding energies is observed, indicating the reduction of scattering rate accompanied by the renormalization effect. While these kink properties are very similar to those reported previously by higher-energy ARPES results, the absolute value of the linewidth is obviously sharper here; $\Delta k\sim0.01$ Å^{-1}. Similar results were recently reported by ARPES experiments using a laser source[16] as well as low-energy synchrotron light,[17] demonstrating the effectiveness and impact of low-energy ARPES for high resolution measurements, not only in energy but also in momentum.

In Figs. 2(a)–2(c), the results of the ultrahigh energy and momentum resolution measurement are shown for UN72K, OP90K, and OV73K. A clear decrease of the linewidth on increasing the doping level is readily visible from the ARPES images. The energy distribution curves (EDCs) (energy spectrum of the ARPES intensity at a fixed momentum) from OV73K, shown in Fig. 2(d), indicate the continuous sharpening of the quasiparticle peak even at binding energies below E_B=10 meV. The quasiparticle peak eventually becomes a sharp peak with 4.2 meV FWHM at $k=k_F$ [red curve in Fig. 2(d)].[18] By fitting the MDCs by Lorentzians, we obtained a clear single band dispersion[20] which is overlaid as a red curve on each image in Figs. 2(a)–2(c). The
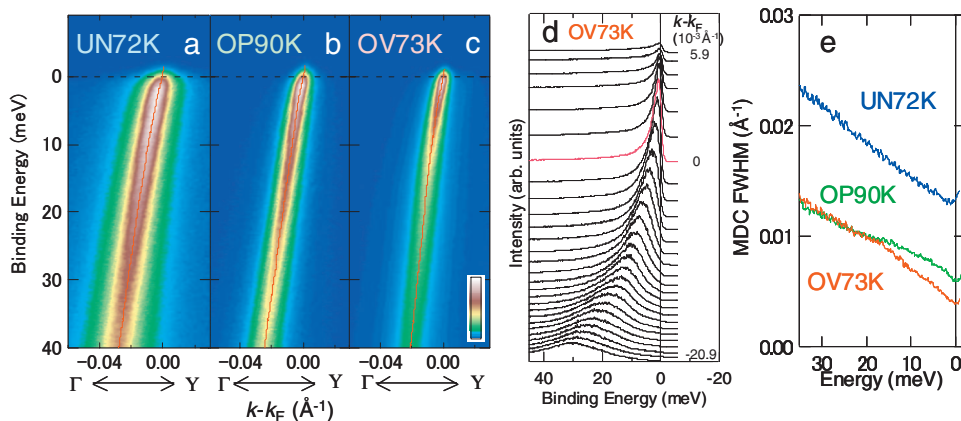

FIG. 2. (Color) [(a)–(c)] Ultrahigh resolution ARPES intensity image plot from Bi2212 UN72K, OP90K, and OV73K, respectively. The red curves show the band dispersions obtained from MDC peak positions. (d) EDC taken from ARPES on OV73K (c). (e) E_B dependence of MDC FWHM obtained from (a) UN72K, (b) OP90K, and (c) OV73K, respectively.
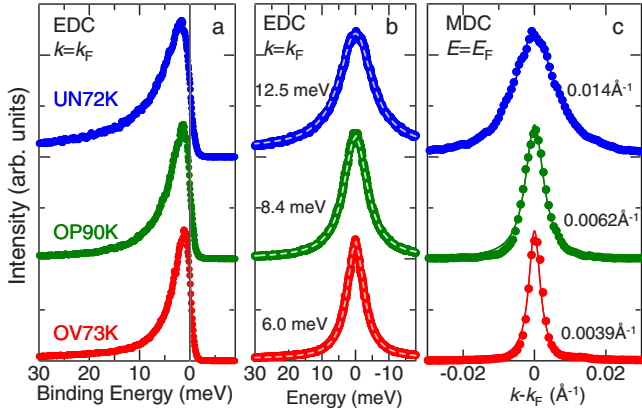
FIG. 3. (Color online) (a) EDC at $k=k_F$ and (b) that symmetrized at E_F from ARPES on Bi2212 UN72K, OP90K, and OV73K [Figs. 2(a)–2(c)]. (c) shows the MDC at $E=E_F$ obtained from the same ARPES spectra. The curves in (b) and (c) are the fitting result by using a single Lorentzian function.

FWHM Δk as a function of E_B is plotted in Fig. 2(e) for UN72K, OP90K, and OV73K. Although the magnitudes of the FWHM Δk are quite similar for OP90K and OV73K (with small differences only at energies below 20 meV), they are significantly higher for the UN72K sample. In spite of these differences, an overall quasilinear ω dependence at low energies is observed for all the samples. Another important observation is that Δk at E_F is significantly doping dependent; $\Delta k(0)=0.014$ Å^{-1} for UN72K reduces to 0.0062 Å^{-1} for OP90K and reduces further to 0.0039 Å^{-1} for OV73K. The corresponding MDCs at E_F and the fitted Lorentzian curves are shown in Fig. 3(c). We can estimate the mean free path l_{mfp} of the nodal quasiparticles from $l_{\mathrm{mfp}}=\Delta k(0)^{-1}$. The estimated values are $l_{\mathrm{mfp}}>260$ Å (OV73K), 160 Å (OP90K), and 70 Å (UN72K). The obtained values of Δk and l_{mfp} for all the samples are shown in Table I. It is noted that these values for the OP90K sample are in very good agreement with the previous works using low-energy incident light.[16,17]

Now, we compare the EDC at k_F among the different doping samples. The EDCs are shown in Fig. 3(a). While the EDC from OV73K shows a clear and sharp peak with very little background, the EDC peak from UN72K apparently tends to become broader. To get rid of the Fermi-Dirac distribution effect at E_F and estimate the FWHM of the peak

from EDCs, we symmetrized them at E_F and plotted them in Fig. 3(b). The symmetrized EDCs can be well fitted with a single Lorentzian function, as shown by the broken curves in Fig. 3(b). The FWHMs obtained from the symmetrized EDCs are 12.5 ± 0.6 (UN72K), 8.4 ± 0.8 (OP90K), and 6.0 ± 0.8 meV (OV73K), where the errors mainly arise from the determination of k_F (see Table I for all samples). The FWHM of an EDC peak corresponds to the scattering rate $\Gamma=h/\tau\approx v_0/v_F\,\mathrm{Im}\,\Sigma$, where τ and v_F correspond to the lifetime and the renormalized Fermi velocity of quasiparticles. The relation between EDC and MDC peak FWHMs can be expressed as $\Gamma\approx v_F\Delta k$, where v_F can be estimated from the gradient of the band dispersion in the vicinity of E_F. By linearly approximating the dispersion at $10\ \mathrm{meV}\leqslant E_B\leqslant 0$ meV obtained from the MDC analysis [red curves in Figs. 2(a)–2(c)], we can get v_F within errors of about $\pm10\%$ and thus Γ from MDCs in Fig. 3(c) as 15 ± 1.4 meV (UN72K), 8.1 ± 0.6 meV (OP90K), and 5.1 ± 0.4 meV (OV73K), which are very similar to the values obtained from EDCs (see Table I). Thus, we succeeded in obtaining the coherent nodal quasiparticle component from ARPES. The observation of the EDC peak obeying a simple Lorentzian curve with almost negligible incoherent part and background provides an important finding that the nodal carriers are well-defined quasiparticles, even in the strongly correlated underdoped region. Regarding its scattering rate Γ estimated from the linewidth, let us compare our results with those from previous transport measurements. The quasiparticle scattering rate obtained from terahertz conductivity using a nearly optimally doped sample ($T_c=85$ K) (Ref. 6) is $1/\tau_{\mathrm{QP}}\sim3$ THz ~12 meV at the lowest temperature of measurement, 12 K. By assuming a simple linear extrapolation, the scattering rate should be $1/\tau_{\mathrm{QP}}\sim2$ THz ~8 meV at around 5 K. This value is equivalent with our result from OP90K (8.1–8.4 meV), indicating full consistency among two completely different probes. While not yet reported, a similar doping-dependence of $1/\tau_{\mathrm{QP}}$ can also be expected in terahertz conductivity measurements on Bi2212.

The doping-dependence of the FWHM Γ thus obtained is plotted in Fig. 4, with that of T_c. Γ shows a monotonic increase from overdoping to underdoping. Such tendency itself is very similar to that of the well-known pseudogap in the $(\pi,0)$ region,[23] being intensively discussed to date as the manifestation of antiferromagnetic spin fluctuation, charge order, phase fluctuation, and so on. Similarly, it is also reported by a previous ARPES study that the linewidth is fairly

TABLE I. Doping-dependence of the nodal quasiparticle property at $\omega=0$. p is the hole concentration estimated from $T_c=T_c^{\mathrm{max}}[1-82.6(0.16-p)^2]$, Δk, l_{mfp}, v_F, and $v_F\Delta k$ are FWHM, mean free path, Fermi velocity, and scattering rate obtained from MDC analysis, and Γ is the scattering rate obtained from EDC analysis (see the text for details).

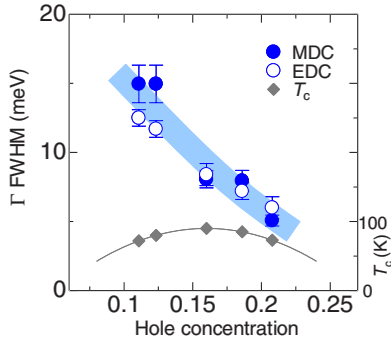| Sample	p	Δk [Å^{-1}]	l_{mfp} [Å]	v_F [eVÅ]	$v_F\Delta k$ [meV]	Γ [meV]
UN72K	0.11	0.0136	74	1.1 (±0.1)	15.0 (±1.4)	12.5 (±0.6)
UN80K	0.12	0.0136	74	1.1 (±0.1)	15.0 (±1.4)	11.7 (±0.6)
OP90K	0.16	0.0062	160	1.3 (±0.1)	8.1 (±0.6)	8.4 (±0.8)
OV85K	0.19	0.0075	130	1.0 (±0.1)	8.0 (±0.8)	7.2 (±0.6)
OV73K	0.21	0.0039	260	1.3 (±0.1)	5.1 (±0.4)	6.0 (±0.8)

FIG. 4. (Color online). Doping-dependence of the scattering rate Γ estimated from the FWHM of EDC and MDC in Bi2212. The right axis shows the T_c of the measured samples with the relation to hole concentration p, $T_c = T_c^{\max}[1 - 82.6(0.16 - p)^2]$.

momentum dependent in underdoped samples, showing that the scattering rate gets greater on approaching $(\pi, 0)$, the pseudogap region, while it is isotropic for overdoped samples.[24] Very recently, systematic investigations of the electronic structures by Raman scattering[25,26] and ARPES[27,28] measurements have revealed that there is a strong dichotomy among the near-nodal (Fermi arc) and the antinodal (pseudogap) regions. The Fermi arc region shows the opening of a well-defined d-wave superconducting gap with coherent quasiparticles regardless of the doping level, while the pseudogap shows a monotonic increase on underdoping with the enhancement of the incoherent spectral shape. Scanning tunneling microscopy (STM) measurements also indicate the spatially inhomogeneous (pseudo)gap spectra arising in the underdoped samples, while keeping rather homogeneous coherent quasiparticle spectra for all doping levels.[29–31] Our observation of the well-defined coherent peaks is basically in agreement with this picture. However, it also shows that the lifetime of the nodal quasiparticle at the center of the Fermi arc shows a significant doping-dependence, when investigated with high energy and momentum resolution at $T = 5$ K.

The lifetime of the nodal quasiparticle can be affected by a number of scattering mechanisms. In the case of a metal with nearly flat density of states (DOS) near E_F, electron-electron scattering can provide the low-energy scattering rate $(\omega \to 0)$ as $\mathrm{Im}\,\Sigma \propto \max(\omega^2, T^2)$ in a Fermi liquid, while $\mathrm{Im}\,\Sigma \propto \max(|\omega|, T)$ in a marginal Fermi liquid picture.[11] Similarly, the electron-phonon scattering gives $\mathrm{Im}\,\Sigma \propto \max(\omega^3, T^3)$. In a d-wave superconducting state, they are completely modified reflecting the $|\omega|$-linear DOS near E_F.[32] The dissipation by electron-electron (or spin fluctuation) scattering is given by $\mathrm{Im}\,\Sigma \propto \max(\omega^3, T^3)$, and electron-phonon scattering by $\mathrm{Im}\,\Sigma \propto \max(\omega^4, T^4)$. In the low energy and temperature limit (appropriate for the present measurements performed at $T \lesssim 0.07 T_c$ with $E_{\mathrm{res}} \sim 1$ meV), however, all the above scattering effects should become negligible. In fact, the ω dependence of the $\mathrm{Im}\,\Sigma \propto \Delta k$ shows a quasilinear

behavior, indicating that the above dissipation mechanisms are not dominant in this T, ω region. One of the remaining terms is the elastic impurity scattering mechanism, which can affect a d-wave superconducting state in a nontrivial way, unlike in a normal metal.[3,33] An in-plane impurity, for example, is known to strongly scatter the quasiparticles and create a localized state around the node appearing as an enhancement of $\mathrm{Im}\,\Sigma(\omega)$ near E_F.[33] In the case of the out-of-plane impurity which likely provides a weak forward scattering potential, on the other hand, $\mathrm{Im}\,\Sigma$ of the quasiparticles can show a $|\omega|$-linear dependence at $\omega \to 0$ with the value of $\mathrm{Im}\,\Sigma(\omega = 0)$ depending on the scattering length of impurity potential and its concentration.[32] Δk showing a ω dependence of convex upward structure at around $E_B = 10$ meV in OP90K may be due to such an elastic scattering, as expected from calculations based on a BCS d-wave model.[32] Recently, the interplay among the apical oxygen dopant, the gap inhomogeneity, and quasiparticle interference has been observed in STM measurements.[34,35] The weakening of the screening effect due to the reduction of carrier density may make the system more susceptible to impurity scattering, typically emerging as granular (typical size of 3 nm) superconductivity in underdoped samples.[29,30] It is interesting that the mean free path of the nodal quasiparticle in UN72K is $l_{\mathrm{mfp}} = 70$ Å, a little bit longer than the reported size of the granular superconducting domains. On the other hand, we cannot yet completely rule out the possibility of the quantum fluctuation enhancement in underdoped samples, such as phase fluctuation arising from the reduction of superfluid density, charge order fluctuation, etc., if they have very low-energy scales ($\lesssim 1$ meV). Future work including detailed temperature-dependent measurements are required to elucidate on these issues.

In conclusion, we have performed an ultrahigh resolution angle-resolved photoemission spectroscopy measurement to elucidate the properties of nodal quasiparticles in a d-wave superconductor. The quasilinear ω dependence of the scattering rate Γ obtained from MDCs suggests the role of an elastic scattering mechanism by out-of-plane impurities, such as oxygen dopants. The value of Γ at $\omega = 0$ for optimally and overdoped samples are 8 and 6 meV, respectively, in a good correspondence with terahertz conductivity results. The doping-dependence of Γ resembles that of the pseudogap, monotonically increasing up to 12 meV on approaching the underdoped region. The estimated mean free paths accordingly decrease from 260 Å in an overdoped to 70 Å in an underdoped sample. This suggests the role of electronic inhomogeneity on the nodal quasiparticle scattering at low temperature in underdoped samples, as is known from STM measurements. The line shapes of EDC and MDC peaks are all well described with single Lorentzian curves, thus indicating validity of a well-defined coherent quasiparticle picture of the nodal carriers covering a wide doping region.

[1] C. C. Tsuei and J. R. Kirtley, Rev. Mod. Phys. **72**, 969 (2000).

[2] A. Damascelli, Z. Hussain, and Z.-X. Shen, Rev. Mod. Phys. **75**, 473 (2003).

[3] A. A. Nersesyan, A. M. Tsvelik, and F. Wenger, Phys. Rev. Lett. **72**, 2628 (1994).

[4] Y. Zhang, N. P. Ong, P. W. Anderson, D. A. Bonn, R. Liang, and W. N. Hardy, Phys. Rev. Lett. **86**, 890 (2001).

[5] A. Hosseini, R. Harris, S. Kamal, P. Dosanjh, J. Preston, R. Liang, W. N. Hardy, and D. A. Bonn, Phys. Rev. B **60**, 1349 (1999).

[6] J. Corson, J. Orenstein, S. Oh, J. O'Donnell, and J. N. Eckstein, Phys. Rev. Lett. **85**, 2569 (2000).

[7] A. Lanzara, P. V. Nogdanov, X. J. Zhou, S. A. Kellar, D. L. Feng, E. D. Lu, T. Yoshida, H. Eisaki, A. Fujimori, K. Kishio, J.-I. Shimoyama, T. Noda, S. Uchida, Z. Hussain, and Z.-X. Shen, Nature (London) **415**, 412 (2002).

[8] G.-H. Gweon, T. Sasagawa, S. Y. Zhou, J. Graf, H. Takagi, D.-H. Lee, and A. Lanzara, Nature (London) **430**, 187 (2004).

[9] J. F. Douglas, H. Iwasawa, Z. Sun, A. V. Fedrov, M. Ishikado, T. Saitoh, H. Eisaki, H. Bando, T. Iwase, A. Ino, M. Arita, K. Shimada, H. Namatame, M. Taniguchi, T. Masui, S. Tajima, K. Fujita, S. Uchida, Y. Aiura, and D. S. Dessau, Nature (London) **446**, 15 (2007).

[10] K. Terashima, H. Matsui, D. Hashimoto, T. Sato, T. Takahashi, H. Ding, T. Yamamoto, and K. Kadowaki, Nat. Phys. **2**, 27 (2006).

[11] C. M. Varma, P. B. Littlewood, S. Schmitt-Rink, E. Abrahams, and A. E. Ruckenstein, Phys. Rev. Lett. **63**, 1996 (1989).

[12] A. A. Kordyuk, S. V. Borisenko, A. Koitzsch, J. Fink, M. Knupfer, B. Buchner, H. Berger, G. Margaritondo, C. T. Lin, B. Keimer, S. Ono, and Y. Ando, Phys. Rev. Lett. **92**, 257006 (2004).

[13] T. Valla, A. V. Fedorov, P. D. Johnson, B. O. Wells, S. L. Hilbert, Q. Li, G. D. Gu, and N. Koshizuka, Science **285**, 2110 (1999).

[14] T. Kiss, F. Kanetaka, T. Yokoya, T. Shimojima, K. Kanai, S. Shin, Y. Onuki, T. Togashi, C. Zhang, C. T. Chen, and S. Watanabe, Phys. Rev. Lett. **94**, 057001 (2005).

[15] T. Mochiku, K. Hirata, and K. Kadowaki, Physica C **282-287**, 475 (1997).

[16] J. D. Koralek, J. F. Douglas, N. C. Plumb, Z. Sun, A. V. Federov, M. M. Murnane, H. C. Kapteyn, S. T. Cundiff, Y. Aiura, K. Oka, H. Eisaki, and D. S. Dessau, Phys. Rev. Lett. **96**, 017005 (2006).

[17] T. Yamasaki, K. Yamazaki, A. Ino, M. Arita, H. Namatame, M. Taniguchi, A. Fujimori, Z.-X. Shen, M. Ishikado, and S. Uchida, Phys. Rev. B **75**, 140513(R) (2007).

[18] We have checked that the narrowness of the peak feature does not arise from a kinematical effect, which may affect the EDC width due to low-energy grazing emission ARPES (Ref. 19). In our case with an emission angle of about 27° and the group velocity (1.0–1.3 eVÅ) obtained from the band dispersion, the kinematical effect does not lead to narrowing but a slight broadening (at most 10%) of the EDC spectral width.

[19] E. D. Hansen, T. Miller, and T.-C. Chiang, Phys. Rev. Lett. **80**, 1766 (1998).

[20] Here, we would like to point out that while recent studies have shown the existence of bilayer splitting at the nodal point (Refs. 17, 21, and 22), we can observe only one band dispersion crossing E_F. The MDC widths obtained for OP90K and OV73K in the present work are smaller than the reported bilayer splitting of 0.0075 Å^{-1}. This indicates that the present result on Bi2212 measures only one of the bilayer split bands, presumably the antibonding band, at the photon energy of the incident laser used in the present study. The spectral weight measured for the bonding and antibonding bands is known to strongly depend on the incident photon energy (Ref. 22).

[21] T. Valla, T. E. Kidd, J. D. Rameau, H.-J. Noh, G. D. Gu, P. D. Johnson, H.-B. Yang, and H. Ding, Phys. Rev. B **73**, 184518 (2006).

[22] A. A. Kordyuk, S. V. Borisenko, A. N. Yaresko, S.-L. Drechsler, H. Rosner, T. K. Kim, A. Koitzsch, K. A. Nenkov, M. Knupfer, J. Fink, R. Follath, H. Berger, B. Keimer, S. Ono, and Y. Ando, Phys. Rev. B **70**, 214525 (2004).

[23] T. Timusk and B. Statt, Rep. Prog. Phys. **62**, 61 (1999).

[24] A. Kaminski, H. M. Fretwell, M. R. Norman, M. Randeria, S. Rosenkranz, U. Chatterjee, J. C. Campuzano, J. Mesot, T. Sato, T. Takahashi, T. Terashima, M. Takano, K. Kadowaki, Z. Z. Li, and H. Raffy, Phys. Rev. B **71**, 014517 (2005).

[25] M. Opel, R. Nemetschek, C. Hoffmann, R. Philipp, P. F. Muller, R. Hackl, I. Tutto, A. Erb, B. Revaz, E. Walker, H. Berger, and L. Forro, Phys. Rev. B **61**, 9752 (2000).

[26] M. L. Tacon, A. Sacuto, A. Georges, G. Kotliar, Y. Gallais, D. Colson, and A. Forget, Nat. Phys. **2**, 537 (2006).

[27] K. Tanaka, W. S. Lee, D. H. Lu, A. Fujimori, T. Hujii, Risdiana, I. Terasaki, D. J. Scalapino, T. P. Devereaux, Z. Hussain, and Z.-X. Shen, Science **314**, 1910 (2006).

[28] T. Kondo, T. Takeuchi, A. Kaminski, S. Tsuda, and S. Shin, Phys. Rev. Lett. **98**, 267004 (2007).

[29] K. M. Lang, V. Madhavan, J. E. Hoffman, E. W. Hudson, H. Eisaki, S. Uchida, and J. C. Davis, Nature (London) **415**, 412 (2002).

[30] K. McElroy, D.-H. Lee, J. E. Hoffman, K. M. Lang, J. Lee, E. W. Hudson, H. Eisaki, S. Uchida, and J. C. Davis, Phys. Rev. Lett. **94**, 197005 (2005).

[31] K. McElroy, R. W. Simmonds, J. E. Hoffman, D.-H. Lee, J. Orenstein, H. Eisaki, S. Uchida, and J. C. Davis, Nature (London) **422**, 592 (2003).

[32] T. Dahm, P. J. Hirschfeld, D. J. Scalapino, and L. Zhu, Phys. Rev. B **72**, 214512 (2005).

[33] P. A. Lee, Phys. Rev. Lett. **71**, 1887 (1993).

[34] K. McElroy, J. Lee, J. A. Slezak, D.-H. Lee, H. Eisaki, S. Uchida, and J. C. Davis, Science **309**, 1048 (2005).

[35] S. Zhou, H. Ding, and Z. Wang, Phys. Rev. Lett. **98**, 076401 (2007).